Journal of Mathematical Modeling
Vol. 13, No. 1, 2025, pp. 49–68. Research Article

JMM

Finite element approximation of coupled Cahn-Hilliard equations with a logarithmic potential and nondegenerate mobility

Ghufran A. Al-Musawi [†,‡], Akil J. Harfash[†*]

[†] *Department of Mathematics, College of Sciences, University of Basrah, Basrah, Iraq*
[‡] *Department of Mathematics, College of Education for Pure Sciences, University of Thi-Qar, Thi-Qar, Iraq*
Email(s): ghufranalmusawi@utq.edu.iq, akil.harfash@uobasrah.edu.iq

Abstract. This research presents a numerical analysis conducted on a system of coupled Cahn-Hilliard equations featuring a logarithmic potential, nondegenerate mobility, and homogeneous Neumann boundary conditions. These equations are derived from a model describing phase separation in a thin film of binary liquid mixture. The study proposes semi-discrete and fully-discrete piecewise linear finite element approximations to the continuous problem. Existence, uniqueness, and various stability estimates for the approximate solutions are established. Fully-discrete error bounds are derived, and optimal time discretisation error is demonstrated. An iterative method is introduced for solving the resulting nonlinear algebraic system, and linear stability analysis in one space dimension is investigated. The research concludes with numerical experiments, providing illustrations of some of the theoretical findings, conducted in both one and two space dimensions.

Keywords: Semi-discrete, logarithmic potential, finite element, weak formulation, error bounds.
AMS Subject Classification 2010: 65M60, 65M15, 65Mxx.

1 Introduction

Various formulations of the Cahn-Hilliard equations have recently attracted considerable attention due to their widespread application in diverse fields, including the modeling of alloys, glasses, and polymers (refer to [10] for examples). Initially developed by Cahn and Hilliard [4] to elucidate the processes involved in splitting a binary mixture into two distinct phases, the Cahn-Hilliard model has proven effective in accurately depicting spinodal decomposition or phase separation phenomena. Numerous qualitative investigations on this subject have been conducted using this classical model (see, for instance, [20]).

*Corresponding author
Received: 4 February 2024 / Revised: 21 August 2024 / Accepted: 9 September 2024
DOI: 10.22124/jmm.2024.26657.2347

In this manuscript, we address the issue of a pair of interlinked Cahn-Hilliard equations characterized by a logarithmic potential, nondegenerate mobility, and homogeneous Neumann boundary conditions. The specific form of the equations is as follows:
Find $\{\phi_1, \phi_2\}$ such that

$$\partial_t \phi_1 = \nabla(M(\phi_1)\nabla w_1), \qquad \text{in} \quad \mathfrak{R}_T, \tag{1}$$

$$\partial_t \phi_2 = \nabla(M(\phi_2)\nabla w_1), \qquad \text{in} \quad \mathfrak{R}_T, \tag{2}$$

where

$$w_1 = \frac{\delta\Lambda(\phi_1,\phi_2)}{\delta\phi_1} = -\gamma\Delta\phi_1 + \Psi_1'(\phi_1) + f_D^{(1)}(\phi_1,\phi_2), \qquad \text{in} \quad \mathfrak{R}_T, \tag{3}$$

$$w_2 = \frac{\delta\Lambda(\phi_1,\phi_2)}{\delta\phi_2} = -\gamma\Delta\phi_2 + \Psi_2'(\phi_2) + f_D^{(2)}(\phi_1,\phi_2), \qquad \text{in} \quad \mathfrak{R}_T, \tag{4}$$

$$\frac{\partial\phi_1}{\partial\nu} = M(\phi_1)\frac{\partial w_1}{\partial\nu} = \frac{\partial\phi_2}{\partial\nu} = M(\phi_2)\frac{\partial w_2}{\partial\nu} = 0, \qquad \text{on} \quad \partial\mathfrak{R}\times(0,T), \tag{5}$$

$$\phi_1(\cdot,0) = \phi_1^0, \qquad \phi_2(\cdot,0) = \phi_2^0 \qquad \text{in} \quad \mathfrak{R}, \tag{6}$$

$$\Psi_i(\mathfrak{s}) = \psi(\mathfrak{s}) + \frac{\theta_i}{2}(1-\mathfrak{s}^2) \quad i=1,2, \quad -1\le\mathfrak{s}\le 1, \quad 0<\theta<\theta_i, \tag{7}$$

$$\psi(\mathfrak{s}) = \frac{\theta}{2}[(1+\mathfrak{s})\ln(1+\mathfrak{s}) + (1-\mathfrak{s})\ln(1-\mathfrak{s})], \tag{8}$$

$$f_D(\mathfrak{s}_1,\mathfrak{s}_2) = D(\mathfrak{s}_1+\sigma_1)^2(\mathfrak{s}_2+\sigma_2)^2, \tag{9}$$

$$f_D^{(i)}(\mathfrak{s}_1,\mathfrak{s}_2) = \frac{\partial f_D(\mathfrak{s}_1,\mathfrak{s}_2)}{\partial\mathfrak{s}_i} = 2D(\mathfrak{s}_i+\sigma_i)(\mathfrak{s}_j+\sigma_j)^2, \quad i,j=1,2, \quad i\neq j, \tag{10}$$

where $\mathfrak{R}$ is an open bounded domain in $\mathbb{R}^n (n=1,2,3)$, $\mathfrak{R}_T = \mathfrak{R}\times(0,T)$, ν represents the outward unit normal to $\partial\mathfrak{R}$, $\delta\Lambda(\phi_1,\phi_2)/\delta\phi_i$, $i=1,2$, denotes the variational derivative of the free energy functional Λ with respect to ϕ_i. The variable ϕ_1 provides information on the local concentration and ϕ_2 indicates the presence of a liquid or a vapor phase. Moreover, $\gamma,\ D,\ \theta,\ \theta_i$ and σ_i are positive constants with $\theta<\theta_i$ and $\Psi_i'(\sigma_i)=0$.

To establish a weak formulation, we multiply by a test function $\chi\in H^1(\mathfrak{R})$ and apply the Green's identity. Further, by a weak solution to the system (1)-(9) we mean that there exists $\{\phi_1,\phi_2,w_1,w_2\}$ satisfying $\phi_1,\phi_2\in L^\infty(0,T;H^1(\mathfrak{R}))\cap H^1(0,T;(H^1(\mathfrak{R}))'), w_1,w_2\in L^2(0,T;H^1(\mathfrak{R}))$ and solving the weak formulation:
(Q) Find $\{\phi_1,\phi_2,w_1,w_2\}\in[H^1(\mathfrak{R})]^4$ such that for a.e. $t\in(0,T),\ \forall i=1,2$ and for all $\chi\in H^1(\mathfrak{R})$:

$$<\partial_t\phi_i,\chi> + (M(\phi_i)\nabla w_i,\nabla\chi) = 0, \tag{11}$$

$$\gamma(\nabla\phi_i,\nabla\chi) + (\Psi_i'(\phi_i),\chi) + (f_D^{(i)}(\phi_1,\phi_2),\chi) = (w_i,\chi). \tag{12}$$

The Cahn-Hilliard equation is formally described as a stiff, fourth-order, nonlinear parabolic partial differential equation. This equation is unique in its ability to represent two simultaneous processes: a rapid phase separation resulting in the creation of thin interfaces between two phases, and a much slower coarsening process leading to the formation of bulk phases separated by these interfaces. Importantly, these two sub-processes operate on distinct time and space scales, presenting a challenge in accurately and efficiently solving the equation within reasonable time constraints and computational resource limits.

Considerable progress has been made in the development of numerical tools for solving the Cahn-Hilliard equation, encompassing both spatial and temporal approximation techniques. The pioneering work of Langer et al. [18] is among the earliest contributions to the numerical study of this equation. Subsequently, various models employing finite difference [22], finite volume [17], finite element [7], and spectral methods [14] have been proposed, each presenting its own set of advantages and limitations. It is noteworthy that a predominant focus has been on addressing two-dimensional problems, with extensive efforts devoted to this aspect. Only recently there has been notable progress in elucidating the three-dimensional morphology evolution of separating phases, particularly from the initial stages until a steady state is attained [9].

In the numerical solution of the Cahn-Hilliard equation, a wide array of time schemes have been employed. These include the widely used Euler-Backward scheme, semi-implicit schemes, and higher-order implicit Runge-Kutta methods. However, recent advancements have introduced adaptive time-stepping schemes as a valuable addition to the toolbox for solving the equation with minimal computational cost. These adaptive schemes leverage rigorous error control, enabling the adjustment of the time step size by several orders of magnitude during the processes of phase separation and coarsening [23]. Recently, the finite element method has been used to solve various physics and engineering problems [11,15,16,19,21].

As demonstrated earlier, the diverse range of applications for the Cahn-Hilliard equation underscores the importance of developing efficient numerical solutions, applicable to fields such as image processing, tumor growth modeling, and the study of phase-separating alloys. For coupled system of Cahn-Hilliard equations with a diffusional mobility depending on ϕ_1, there are still mathematical and numerical work which has been done in this paper. By considering system (1)-(10), with a diffusional mobility $M(\phi_1)$ depending on ϕ_1, many mathematical problems have been treated in this article. The mathematical treatments used in this article can be the basis for treating many mathematical problems that may arise in the analysis of numerical solutions to various mathematical and physical problems. In this paper, we put forth a highly efficient linear finite element approach tailored for solving coupled Cahn-Hilliard equations featuring a logarithmic potential and nondegenerate mobility.

The initial section of the article outlines a semi-discrete method for approximating the solution of the continuous problem denoted as (Q). This involves discretization in the spatial variable using a linear finite element method. In Section 2, essential notations are introduced, which will be employed throughout the manuscript. Section 3 presents fundamental tools and results related to the piecewise linear finite element space. The following Section 4 introduces a regulated variant of the continuous problem (Q). It proceeds to express both the original problem (Q) and its regulated counterpart in equivalent formulations. In Section 5, a semi-discrete approximation to the solution of the regulated problem is formulated, involving spatial variable discretization through a finite element method. The existence of the proposed semi-discrete approximation is then established in Section 5.1. In Section 6, we establish a fully-discrete linear finite element approximation for the continuous problem, incorporating symmetry in the temporal domain. The discretization in time is achieved through the backward Euler method. The investigation of the fully-discrete problem involves the consideration of a regularized version, for which the existence of a solution is proven using Schauders fixed point theorem. Notably, there are no constraints imposed on the mesh parameter or time step, as detailed in Section 6.1. Additionally, Section 7, delves into numerical experiments conducted in one and two dimensions, serving to validate the previously derived theoretical results and explore the growth behavior of solutions. All simulations were executed using programs written in the Matlab programming language. In 7.1.1, we present a practical algorithm for computing the numerical solution, and in Section 7.1, we discuss computational results pertaining to the fully-discrete error bound in one and two dimensions. Finally, 7.3 showcases two-dimensional simulations.

2 Notation and preliminaries

Firstly, the mean integral can be defined in the following way:

$$\fint \zeta = \frac{1}{|\mathfrak{R}|}(\zeta, 1), \quad \forall \zeta \in L^1(\mathfrak{R}). \tag{13}$$

We can conveniently introduce the "inverse Laplacian Green's operator" denoted as $\mathscr{G} : \mathscr{F}_0 \to V_0$ in a manner that

$$(\nabla \mathscr{G} f, \nabla \eta) = \langle f, \eta \rangle, \quad \forall \eta \in H^1(\mathfrak{R}), \tag{14}$$

where $\mathscr{F}_0 = \{f \in (H^1(\mathfrak{R}))' : \langle f, 1 \rangle = 0\}$, $V_0 = \{v \in H^1(\mathfrak{R}) : (v, 1) = 0\}$, and $\langle \cdot, \cdot \rangle$ denotes the duality pairing between $(H^1(\mathfrak{R}))'$ and $H^1(\mathfrak{R})$ such that

$$\langle f, \eta \rangle = (f, \eta), \quad \forall f \in L^2(\mathfrak{R}) \ \ \textit{and} \ \ \eta \in H^1(\mathfrak{R}). \tag{15}$$

The well-posedness of $\mathscr{G}$ can be derived from the Lax-Milgram theorem, coupled with the application of the Poincare inequality, as illustrated in various references [5]

$$|\rho|_0 \le C_p(|\rho|_1 + |(\rho, 1)|), \ \ \forall \rho \in H^1(\mathfrak{R}). \tag{16}$$

It can be deduced from equations (15) and (16) that, for any $\rho \in L^2(\mathfrak{R}) \cap \mathscr{F}_0$,

$$\|\rho\|_{-1}^2 = \langle \rho, \mathscr{G} v \rangle = (\rho, \mathscr{G}\rho) \le \|\rho\|_0 \|\mathscr{G}\rho\|_0 \le C_p \|\rho\|_0 |\mathscr{G}\rho|_1 = C_p \|\rho\|_0 \|\rho\|_{-1} \tag{17}$$

which implies that

$$\|\rho\|_{-1} \le C_p \|\rho\|_0. \tag{18}$$

Furthermore, we obtain that

$$\|\theta\|_{(H^1(\mathfrak{R}))'} = \sup_{\|\rho\|_1 = 1} |\langle \theta, \rho \rangle| = \sup_{\|\rho\|_1 = 1} |(\nabla \mathscr{G}\theta, \nabla \rho)| \le \sup_{\|\rho\|_1 = 1} \|\theta\|_{-1} |\rho|_1 \le \|\theta\|_{-1}. \tag{19}$$

Additionally, we require the following outcome as presented in [5]:

$$H^1(\mathfrak{R}) \overset{c}{\hookrightarrow} L^\rho(\mathfrak{R}) \hookrightarrow (H^1(\mathfrak{R}))' \text{ holds for } \rho \in \begin{cases} [1, \infty], & \text{if } d = 1, \\ [1, \infty), & \text{if } d = 2, \\ [1, 6], & \text{if } d = 3. \end{cases} \tag{20}$$

3 Finite element spaces and associated results

In the forthcoming sections, we will delve into the examination of semi-discrete and fully-discrete linear finite element approximations for the problem (Q), subject to the following assumptions on the mesh:

(A_1) Let $\{\phi_1^0, \phi_2^0\} \in H^1(\mathfrak{R}) \times H^1(\mathfrak{R})$ such that $\max\{|\phi_1^0|_{0,\infty}, |\phi_2^0|_{0,\infty}\} \le 1$ and for some given $\delta_0 \in (0, 1), \max\{|m_1| = |\fint \phi_1^0|, |m_2| = |\fint \phi_2^0|\} \le 1 - \delta_0$.

(A^h) Let $\mathfrak{R} \subset \mathbb{R}^d$, where $d \leq 3$, represents a convex polygonal or polyhedral domain for $d = 2$ or $d = 3$. Consider $\mathscr{T}^h$ as a quasi-uniform partition of $\mathfrak{R}$ comprising disjoint open simplices τ^1, where h_τ denotes the diameter of τ, and $h = \max_{\tau \in \mathscr{T}^h} h_\tau$. This partition ensures that $\bar{\mathfrak{R}} = \cup_{\tau \in \mathscr{T}^h} \bar{\tau}$. Additionally, we assume that $\mathscr{T}^h$ is weakly acute, as per the definition by Barrett and Blowey, indicating that for (i) $d = 2$, the sum of opposite angles relative to any side does not exceed π, and for (ii) $d = 3$, the angle between any two faces of the tetrahedron does not exceed $\frac{\pi}{2}$.

Connected to $\mathscr{T}^h$, we now define the standard finite element space, which comprises continuous piecewise linear functions. Let $S^h \subset H^1(\mathfrak{R})$ be a finite element space defined by

$$S^h = \{\omega \in C(\overline{\mathfrak{R}}) : \omega|_\tau \text{ is linear } \forall \tau \in \mathscr{T}^h\}.$$

Recalling that $m_i := \fint u_0^i$ it is also convenient to introduce for $i = 1,2$

$$S^h_{m_i} := \{\chi \in S^h : \fint \chi = m_i\}.$$

Let $\{x_i\}_{i=1}^J$ represent the set of nodes in τ^h, and $\{\eta_i\}_{i=1}^J$ be a basis of S^h defined by $\eta_i(x_j) = \delta_{ij}$, for $i, j = 1, \ldots, J$. Consider $\pi^h : C(\overline{\mathfrak{R}}) \mapsto S^h$ as the Lagrange interpolation operator, such that $\pi^h \omega(x_i) = \omega(x_i)$ for $i = 1, \ldots, J$. Define a discrete L^2 inner product on $C(\overline{\mathfrak{R}})$ as follows:

$$(\omega_1, \omega_2)^h = \int_{\mathfrak{R}} \pi^h\{\omega_1(x)\omega_2(x)\} d\mathbf{x} \equiv \sum_{i=1}^J m_i \omega_1(x_i)\omega_2(x_i), \tag{21}$$

where $m_i = (\varphi(\eta_i), \varphi(\eta_i))^h = (1, \varphi(\eta_i)) > 0$ which is called the lumped mass matrix.

We can demonstrate that

$$(\pi^h \omega_1, \omega_2)^h := (\omega_1, \omega_2)^h,\ \forall \omega_1, \omega_2 \in C(\overline{\mathfrak{R}}),\ \text{ and } (\omega, 1)^h := (\omega, 1),\ \forall \omega \in S^h. \tag{22}$$

Additionally, we define $K_{ij} := (\nabla\varphi_i, \nabla\varphi_j)$. The norm induced by $|\cdot|_h = [(\cdot,\cdot)^h]^{\frac{1}{2}}$ on S^h is equivalent to $|\cdot|_0 = [(\cdot,\cdot)]^{\frac{1}{2}}$. The following results concerning the space S^h are needed, as detailed in [6]:

$$C_1\|\omega\|_0 \leq |\omega|_h \leq C_2\|\omega\|_0, \quad \forall \omega \in S^h. \tag{23}$$

For sufficiently small h, the discrete Poincare inequality takes the form

$$((\xi,\xi)^h)^{\frac{1}{2}} = |\xi|_h \leq C_p(|\xi|_1 + |(\xi,1)^h|). \tag{24}$$

For all $\varsigma(x) \in S^h$, we define that:

$$|\varsigma^h|_{h,r} := \Big(\int_{\mathfrak{R}} \pi^h\{|\varsigma(x)^h|^r\} d\mathbf{x}\Big)^{\frac{1}{r}} \equiv \Big(\sum_{i=0}^k \widehat{M}_{jj} |\varsigma(x_i)^h|^r\Big)^{\frac{1}{r}}, \quad \text{if } 0 \leq r < \infty, \tag{25}$$

$$|\varsigma^h|_{h,\infty} := \max_{0\leq j\leq k} |\varsigma(x_j)^h|, \qquad \text{if } r = \infty. \tag{26}$$

In a manner akin to (14), we present the operator $\hat{\mathscr{G}}^h : \mathscr{F}^h \to V^h$, where

$$(\nabla\hat{\mathscr{G}}^h v, \nabla\chi) = (v,\chi)^h,\ \forall \chi \in S^h, \tag{27}$$

$$V^h = \{v^h \in S^h : (v^h, 1) = 0\},$$

$$\mathscr{F}^h = \{v \in C(\mathfrak{R}) : (v,1)^h = 0\}. \tag{28}$$

For later purpose, we introduce the following inverse inequalities which follow from the quasi-uniform condition

$$|\chi|_{m,q} \le Ch^{d(\frac{1}{q}-\frac{1}{p})}|\chi|_{m,p}, \quad 1 \le p \le q \le \infty, \;\; m = 0,1, \;\forall \chi \in S^h, \tag{29}$$

$$|\chi|_1 \le \frac{C}{h}|\chi|_h, \;\; \forall \chi \in S^h. \tag{30}$$

We also acknowledge the following inequalities (refer to [3]):

$$C_1 h^2 |\eta|_1 \le C_2 h \|\eta\|_0 \le \|\eta\|_{-h} \le \|\eta\|_{-1} \le C_3 \|\eta\|_{-h}, \;\; \forall \eta \in V^h. \tag{31}$$

To handle the initial data in both the semi-discrete and fully-discrete approximations, we introduce the weighted H^1-projection (cf. Barrett and Blowey, [2] $P^h_\gamma : H^1 \to S^h$), defined as:

$$\gamma(\nabla(I - P^h_\gamma)\omega_1, \nabla\omega_2) + ((I - P^h_\gamma)\omega_1, \omega_2) = 0, \;\; \forall \omega_2 \in S^h, \tag{32}$$

and we also revisit the discrete L^2-projection (refer to, for instance, [3], denoted as $P^h : L^2 \mapsto S^h$, which is defined as:

$$(P^h \nu, \omega^k)^h = (\nu, \omega^k) \quad \text{for all} \;\; \nu \in L^2, \; \omega^k \in S^h. \tag{33}$$

The aforementioned projections fulfill the subsequent crucial outcomes (e,g. [3])

$$|(I - P^h)\eta|_m \le Ch^{1-m}|\eta|_1, \quad m = 0,1, \;\; \forall \;\eta \;\; \in H^1, \tag{34}$$

$$|P^h \eta|_{0,\infty} \le |\eta|_{0,\infty}, \quad\;\; \forall \eta \in L^\infty. \tag{35}$$

The following property of projection is also required:

$$\|P^h \omega\|_1 \le C\|\omega\|_1, \;\; \forall \omega \in H^1. \tag{36}$$

For $\chi, v \in C(\overline{\mathfrak{R}})$, the following holds:

$$(\chi, v)^h \equiv \int_{\mathfrak{R}} \pi^h(\chi v)dx \le \Big(\int_{\mathfrak{R}} \pi^h(|\chi|^p)dx\Big)^{\frac{1}{p}} \Big(\int_{\mathfrak{R}} \pi^h(|v|^q)dx\Big)^{\frac{1}{q}}, \text{ where } \frac{1}{p} + \frac{1}{q} = 1, p, q \ge 1, \tag{37}$$

$$(\chi^r, 1)^h \equiv \int_{\mathfrak{R}} \pi^h(\chi^r)dx \le C\|\chi\|_1^r \text{ holds for } r \in \begin{cases} [2,\infty], & \text{if } d = 1,2, \\ [2,6], & \text{if } d = 3. \end{cases} \text{ for each } \chi \in S^h \text{ and } r \ge 2. \tag{38}$$

4 The regularization and equivalent weak formulations

We employ a regularization technique described in [8], involving the introduction of a twice continuously differentiable function denoted as $\Theta_\varepsilon \in C^2(\mathbb{R})$, where $\varepsilon \in (0,1)$. The function is defined as:

$$\Theta_\varepsilon(\mathfrak{s}) = \begin{cases} \frac{\theta}{4\varepsilon}\mathfrak{s}^2 + \frac{\theta}{2}\mathfrak{s}\ln\varepsilon - \frac{\theta\varepsilon}{4}, & \text{if } \mathfrak{s} \le \varepsilon, \\ \Theta(\mathfrak{s}) \equiv \frac{\theta}{2}\mathfrak{s}\ln\mathfrak{s}, & \text{if } \mathfrak{s} \ge \varepsilon. \end{cases} \tag{39}$$

Following that, we proceed to define the function $\psi_\varepsilon \in C^2(R)$ in the following manner:

$$\psi_\varepsilon(\mathfrak{s}) = \Theta_\varepsilon(1+\mathfrak{s}) + \Theta_\varepsilon(1-\mathfrak{s}) = \begin{cases} \Theta(1+\mathfrak{s}) + \Theta_\varepsilon(1-\mathfrak{s}), & \text{if } \mathfrak{s} \geq 1-\varepsilon, \\ \psi(\mathfrak{s}) \equiv \Theta(1+\mathfrak{s}) + \Theta(1-\mathfrak{s}), & \text{if } |\mathfrak{s}| \leq 1-\varepsilon, \\ \Theta_\varepsilon(1+\mathfrak{s}) + \Theta(1-\mathfrak{s}), & \text{if } \mathfrak{s} \leq -1+\varepsilon. \end{cases} \tag{40}$$

Therefore, for $i = 1,2$, we incorporate regularization into the potential Ψ_i by introducing $\Psi_{\varepsilon,i} \in C^2(R)$ in such a way that:

$$\Psi_{\varepsilon,i}(\mathfrak{s}) = \psi_\varepsilon(\mathfrak{s}) + \frac{\theta_i}{2}(1-\mathfrak{s}^2). \tag{41}$$

Furthermore, we introduce the monotone odd function $\Xi_\varepsilon : \mathbb{R} \to \mathbb{R}$ in the following expression:

$$\Xi_\varepsilon(\mathfrak{s}) = \psi_\varepsilon'(\mathfrak{s}) = \begin{cases} \Theta'(1+\mathfrak{s})\Theta_\varepsilon'(1-\mathfrak{s}), & \text{if } \mathfrak{s} \geq 1-\varepsilon, \\ \psi'(\mathfrak{s}) \equiv \Xi(\mathfrak{s}) \equiv \Theta'(1+\mathfrak{s}) - \Theta'(1-\mathfrak{s}), & \text{if } |\mathfrak{s}| \leq 1-\varepsilon, \\ \Theta_\varepsilon'(1+\mathfrak{s}) - \Theta'(1-\mathfrak{s}), & \text{if } \mathfrak{s} \leq -1+\varepsilon. \end{cases} \tag{42}$$

Here, we will outline certain characteristics of the aforementioned functions that will be referenced throughout the article. The lemma presented below reveals important results regarding $\Psi_{\varepsilon,i}$, Ξ, and Ξ_ε.

Lemma 1 ([2,3])**.**

$$\forall\ \varepsilon \leq \varepsilon_0 := \min\{\frac{\theta}{4\theta_1}, \frac{\theta}{4\theta_2}\}, \Psi_{\varepsilon,i}(\mathfrak{s}) \geq -\frac{8\theta_i^2+\theta^2}{16\theta_i} = -C_0, \quad i = 1,2, \quad \mathfrak{s} \in \mathbb{R}, \tag{43}$$

$$|\Xi_\varepsilon^{-1}(\mathfrak{s}) - \Xi^{-1}(\mathfrak{s})| \leq \frac{2\varepsilon}{\theta}\Big([\mathfrak{s} - \Xi(1-\varepsilon)]_+ + [-\mathfrak{s} - \Xi(1-\varepsilon)]_+\Big),\ \mathfrak{s} \in \mathbb{R}, \tag{44}$$

where $[\cdot]_+ = \max\{\cdot, 0\}$.

Lemma 2 ([2,3])**.** *Suppose $\mathscr{T}^h$ represents a weakly acute partition, and let $\varepsilon = \frac{1}{2}$, then we have that*

$$\|\pi^h \Xi_\varepsilon(\chi)\|_0^2 \leq \frac{\theta}{\varepsilon}(\nabla\chi, \nabla\pi^h\Xi_\varepsilon(\chi)), \quad \forall \chi \in S^h. \tag{45}$$

Further, if $|\chi|_{0,\infty} \leq 1-\varepsilon$, *then*

$$\|\nabla\pi^h\Xi_\varepsilon(\chi)\|_0^2 \leq \Xi'(|\chi|_{0,\infty})(\nabla\chi, \nabla\pi^h\Xi_\varepsilon(\chi)), \tag{46}$$

where $[\cdot]_+ = \max\{\cdot, 0\}$.

Next, we present a regularized version denoted as (Q_ε) for the original (Q):
(Q_ε) Find $\{\phi_{\varepsilon,1}, \phi_{\varepsilon,2}, w_{\varepsilon,1}, w_{\varepsilon,2}\} \in [H^1(\mathfrak{R})]^4$ such that for i=1, 2, $\phi_{\varepsilon,i}(0) = \phi_i(0)$ and for a.e. $t \in (0,T)$ and all $\chi \in H^1(\mathfrak{R})$

$$(\partial_t\phi_{\varepsilon,i}, \chi) = -(M(\phi_{\varepsilon,i})\nabla w_{\varepsilon,i}, \nabla\chi), \tag{47}$$

$$(w_{\varepsilon,i}, \chi) = \gamma(\nabla\phi_{\varepsilon,i}, \nabla\chi) + (\Psi'_{\varepsilon,i}(\phi_{\varepsilon,i}), \chi) + (f_D^{(i)}(\phi_{\varepsilon,1}, \phi_{\varepsilon,2}), \chi). \tag{48}$$

5 A semi-discrete approximation

We consider the following semi-discrete linear finite element approximations to the problems (Q) and (Q_ε), respectively:
(Q^h) Find $\{\phi_1^h, \phi_2^h, w_1^h, w_2^h\} \in S^h \times S^h \times S^h \times S^h$ such that for $a.e.\ t \in (0,T)$

$$(\partial_t \phi_i^h, \chi^h)^h = -(M(\phi_i^h)\nabla w_i^h, \nabla \chi^h), \tag{49}$$

$$(w_i^h, \chi^h)^h = \gamma(\nabla \phi_i^h, \nabla \chi^h) + (\Psi_i'(\phi_i^h), \chi^h)^h + (f_D^{(i)}(\phi_1^h, \phi_2^h), \chi^h)^h, \tag{50}$$

$$\phi_i^h(x,0) = P^h \phi_i^0(x), \tag{51}$$

where $\Psi_i'(\cdot)$ and $f_D^{(i)}(\cdot,\cdot)$ are given by (7) and (9), respectively.

We examine the subsequent semi-discrete linear finite element approximation for the problem (Q_ε):
(Q_ε^h) Find $\{\phi_{\varepsilon,1}^h, \phi_{\varepsilon,2}^h, w_{\varepsilon,1}^h, w_{\varepsilon,2}^h\} \in [H^1(\mathfrak{R})]^4$ such that for $i = 1,2$, $\phi_{\varepsilon,i}^h(0) = P^h \phi_i^0$ and for a.e. $t \in (0,T)$ and all $\chi^h \in H^1(\mathfrak{R})$

$$(\partial_t \phi_{\varepsilon,i}^h, \chi^h)^h = -(M(\phi_{\varepsilon,i}^h)\nabla w_{\varepsilon,i}^h, \nabla \chi^h), \tag{52}$$

$$(w_{\varepsilon,i}^h, \chi^h)^h = \gamma(\nabla \phi_{\varepsilon,i}^h, \nabla \chi^h) + (\Psi_{\varepsilon,i}'(\phi_{\varepsilon,i}^h), \chi^h)^h + (f_D^{(i)}(\phi_{\varepsilon,1}^h, \phi_{\varepsilon,2}^h), \chi^h)^h, \tag{53}$$

where $\Psi_i'(\cdot)$ and $f_D^{(i)}(\cdot,\cdot)$ are given by (7) and (9), respectively.

To establish equivalent forms for (Q^h) and ($\mathrm{Q}\varepsilon^h$), we set $\chi^h = 1$ in (52). This yields, for $i = 1,2$ and $t \in (0,T)$, that $\partial t \phi_{\varepsilon,i}^h \in V_0^h$. Additionally, if $\phi_i^{h,0} = P_\gamma^h \phi_i^0$, then based on (22) and (32), we have that

$$(\phi_{\varepsilon,i}^h(t), 1) \equiv (\phi_{\varepsilon,i}^h(t), 1)^h = (\phi_{\varepsilon,i}^h(0), 1)^h = (\phi_{\varepsilon,i}^h(0), 1) = (P_\gamma^h \phi_i^0, 1) = (\phi_i^0, 1) = m_i|\mathfrak{R}|. \tag{54}$$

Similarly, in the scenario where $\phi_i^{h,0} = P^h \phi_i^0$, we deduce from (33) that

$$(\phi_{\varepsilon,i}^h(t), 1) \equiv (\phi_{\varepsilon,i}^h(t), 1)^h = (P^h \phi_i^0, 1)^h = (\phi_i^0, 1) = m_i|\mathfrak{R}|. \tag{55}$$

5.1 Global existence of the of the semi-discrete approximation

Theorem 1. *Assuming that* (A_1) *and* (A^h) *are valid, and defining* $\phi_i^{h,0}$ *as* $P^h \phi_i^0$*, then, for any* $\varepsilon < \varepsilon_0$ *and* $h > 0$*, the problem denoted as* (Q^h) *has a solution* $\phi_{\varepsilon,1}^h, \phi_{\varepsilon,2}^h, w_{\varepsilon,1}^h, w_{\varepsilon,2}^h$*. These solutions satisfy the following stability estimates, for* $i = 1,2$*, and these estimates remain independent of the parameters* ε *and* h*,*

$$\|\phi_{\varepsilon,i}^h\|_{L^\infty(0,T;(H^1(\mathfrak{R})))} + \|\phi_{\varepsilon,i}^h\|_{H^1(0,T;(H^1(\mathfrak{R}))')} \le C, \tag{56}$$

$$\|w_{\varepsilon,i}^h\|_{L^2(0,T;H^1(\mathfrak{R}))} \le C, \tag{57}$$

$$\|\partial_t \phi_{\varepsilon,i}^h\|_{L^2(0,T;(H^1(\mathfrak{R}))')} \le C, \tag{58}$$

$$\|\pi^h f_D^{(i)}(\phi_{\varepsilon,1}^h, \phi_{\varepsilon,2}^h)\|_{L^\infty(0,T,L^2(\mathfrak{R}))} \le C, \tag{59}$$

$$\|\pi^h \Xi_\varepsilon(\phi_{\varepsilon,i}^h)\|_{L^2(\mathfrak{R}_T)} \le C. \tag{60}$$

Proof. Next, let us explore the given free energy in the following format:

$$
\begin{aligned}
E(\phi^h_{\varepsilon,1},\phi^h_{\varepsilon,2}) =& \frac{\gamma}{2}\|\nabla\phi^h_{\varepsilon,1}\|_0^2+\frac{\gamma}{2}\|\nabla\phi^h_{\varepsilon,2}\|_0^2+(\Psi_{\varepsilon,1}(\phi^h_{\varepsilon,1}),1)^h+(\Psi_{\varepsilon,2}(\phi^h_{\varepsilon,2}),1)^h\\
&+(f_D(\phi^h_{\varepsilon,1},\phi^h_{\varepsilon,2}),1)^h,
\end{aligned}
\tag{61}
$$

where $\Psi(\cdot)$ and $f_D(\cdot,\cdot)$ are given by (7) and (9), respectively. Taking the derivative of $E(\phi^h_{\varepsilon,1},\phi^h_{\varepsilon,2})$ with respect to t and utilizing (9) and (21) results in

$$
\begin{aligned}
\partial_t E\left(\phi^h_{\varepsilon,1},\phi^h_{\varepsilon,2}\right) =& \gamma\left(\nabla\phi^h_{\varepsilon,1},\nabla\partial_t\phi^h_{\varepsilon,1}\right)+\gamma\left(\nabla\phi^h_{\varepsilon,2},\nabla\partial_t\phi^h_{\varepsilon,2}\right)\\
&+\left(\Psi'_{\varepsilon,1}(\phi^h_{\varepsilon,1}),\partial_t\phi^h_{\varepsilon,1}\right)^h+\left(\Psi'_{\varepsilon,2}(\phi^h_{\varepsilon,2}),\partial_t\phi^h_{\varepsilon,2}\right)^h\\
&+\left(f_D^{(1)}(\phi^h_{\varepsilon,1},\phi^h_{\varepsilon,2}),\partial_t\phi^h_{\varepsilon,1}\right)^h+\left(f_D^{(2)}(\phi^h_{\varepsilon,1},\phi^h_{\varepsilon,2}),\partial_t\phi^h_{\varepsilon,2}\right)^h.
\end{aligned}
\tag{62}
$$

Substituting $\chi^h = w^h_{\varepsilon,1}$ into (52) and $\chi^h=\partial_t\phi^h_{\varepsilon,i}$ into (53), we can represent (62) for each $i=1,2$ as follows:

$$
-\int_{\mathfrak{R}} M(\phi^h_{\varepsilon,i})|\nabla w^h_{\varepsilon,i}|^2 d\mathbf{x} = \gamma(\nabla\phi^h_{\varepsilon,i},\nabla\partial_t\phi^h_{\varepsilon,1})+(\Psi'_{\varepsilon,i}(\phi^h_{\varepsilon,i}),\partial_t\phi^h_{\varepsilon,1})^h+(f_D^{(i)}(\phi^h_{\varepsilon,1},\phi^h_{\varepsilon,2}),\partial_t\phi^h_{\varepsilon,i})^h. \tag{63}
$$

Substituting (63) into (62) for $i=1,2$, yields that

$$
\begin{aligned}
\partial_t E(\phi^h_{\varepsilon,1},\phi^h_{\varepsilon,2}) =& -\int_{\mathfrak{R}} M(\phi^h_{\varepsilon,1})|\nabla w^h_{\varepsilon,1}|^2 d\mathbf{x}-\int_{\mathfrak{R}} M(\phi^h_{\varepsilon,2})|\nabla w^h_{\varepsilon,2}|^2 d\mathbf{x}\\
=& -\sum_{i=1}^{2}\int_{\mathfrak{R}} M(\phi^h_{\varepsilon,i})|\nabla w^h_{\varepsilon,i}|^2 d\mathbf{x}\le 0.
\end{aligned}
\tag{64}
$$

Hence, E functions as a Lyapunov functional. Integrating (64) over $t\in(0,T)$ and considering (51) for each $i=1,2$, it can be concluded that

$$
E(\phi^h_{\varepsilon,1}(t),\phi^h_{\varepsilon,2}(t))+\int_{\mathfrak{R}_T}[M(\phi^h_{\varepsilon,1})|\nabla w^h_{\varepsilon,1}|^2+M(\phi^h_{\varepsilon,2})|\nabla w^h_{\varepsilon,2}|^2]d\mathbf{x}dt\le E(P^h\phi_1^0,P^h\phi_2^0). \tag{65}
$$

In (61), when substituting $\phi^h_{\varepsilon,i}=P^h\phi_i^0$ for $i=1,2$, we obtain that

$$
\begin{aligned}
E(P^h\phi_1^0,P^h\phi_2^0) =& \int_{\mathfrak{R}}\Big[\frac{\gamma}{2}|\nabla P^h\phi_1^0|^2+\pi^h\Psi_{\varepsilon,1}(P^h\phi_1^0)+\frac{\gamma}{2}|\nabla P^h\phi_2^0|^2\\
&+\pi^h\Psi_{\varepsilon,2}(P^h\phi_2^0)+\pi^h f_D(P^h\phi_1^0,P^h\phi_2^0)]d\mathbf{x}.
\end{aligned}
\tag{66}
$$

Now, we bound each terms of (66) in turn. From (34) and the assumptions (A_1), we have for $i=1,2$ that

$$
\|P^h\phi_i^0\|_1\le C\|\phi_i^0\|_1\le C, \tag{67}
$$

Utilizing (35) and the given assumptions (A_1), for $i=1,2$, we also have:

$$
\|P^h\phi_i^0\|_{0,\infty}\le|\phi_i^0|_{0,\infty}\le 1.
$$

Using the fact that $\psi_\varepsilon(r) \le \psi_\varepsilon(1), \ \ \forall\, r \ \in [-1,1]$, it follows, for $i=1,2$, that

$$(\Psi_{\varepsilon,i}(P^h\phi_i^0),1)^h \le (\psi_\varepsilon(1)+\frac{\theta_i}{2},1)^h \le (\theta\ln 2+\frac{\theta_i}{2})|\mathfrak{R}|. \tag{68}$$

We utilize (37) and (38) to bound $f_D(P^h\phi_1^0,P^h\phi_2^0)$ in the following manner:

$$\begin{aligned}(f_D(P^h\phi_1^0,P^h\phi_2^0),1)^h =& D\int_{\mathfrak{R}} \pi^h\Big((P^h\phi_1^0+\alpha_1)^2(P^h\phi_2^0+\alpha_2)^2\Big)dx\\ \le& C[\|\phi_1^0\|_1^2+1][\|\phi_2^0\|_1^2+1] \le C,\end{aligned} \tag{69}$$

where we have also used (38) and the assumptions (A_1). Bringing together the estimates (67)-(69) along with (66), we find that

$$E(P^h\phi_1^0,P^h\phi_2^0) \le C. \tag{70}$$

Therefore, by combining (70) and (65), it follows that

$$E(\phi_{\varepsilon,1}^h(t),\phi_{\varepsilon,2}^h(t))+\int_{\mathfrak{R}_T}[M(\phi_{\varepsilon,1}^h)|\nabla w_{\varepsilon,1}^h|^2+M(\phi_{\varepsilon,2}^h)|\nabla w_{\varepsilon,2}^h|^2]d\mathbf{x}dt \le C. \tag{71}$$

Substituting (61) into (71), we obtain that

$$\begin{aligned}&\frac{\gamma}{2}\|\nabla\phi_{\varepsilon,1}^h\|_0^2+\frac{\gamma}{2}\|\nabla\phi_{\varepsilon,2}^h\|_0^2+(\Psi_{\varepsilon,1}(\phi_{\varepsilon,1}^h),1)^h+(\Psi_{\varepsilon,2}(\phi_{\varepsilon,2}^h),1)^h+(f_D(\phi_{\varepsilon,1}^h,\phi_{\varepsilon,2}^h),1)^h\\ &\qquad+\int_{\mathfrak{R}_T}[M(\phi_{\varepsilon,1}^h)|\nabla w_{\varepsilon,1}^h|^2+M(\phi_{\varepsilon,2}^h)|\nabla w_{\varepsilon,2}^h|^2]d\mathbf{x}dt \le C.\end{aligned}$$

Given that the functions $\Psi_{\varepsilon,i}(\phi_{\varepsilon,i}^h)$ and $f_D(\phi_{\varepsilon,1}^h,\phi_{\varepsilon,2}^h)$ are positive for each $i=1,2$, we conclude

$$\frac{\gamma}{2}\|\nabla\phi_{\varepsilon,1}^h\|_0^2+\frac{\gamma}{2}\|\nabla\phi_{\varepsilon,2}^h\|_0^2+\int_{\mathfrak{R}_T}[M(\phi_{\varepsilon,1}^h)|\nabla w_{\varepsilon,1}^h|^2+M(\phi_{\varepsilon,2}^h)|\nabla w_{\varepsilon,2}^h|^2]d\mathbf{x}dt \le C. \tag{72}$$

From (72), we deduce that

$$\frac{\gamma}{2}|\phi_{\varepsilon,1}^h|_1^2+\frac{\gamma}{2}|\phi_{\varepsilon,2}^h|_1^2+\int_T\Big[([M(\phi_{\varepsilon,1}^h)]^{\frac{1}{2}}|\nabla w_{\varepsilon,1}^h|)^2+([M(\phi_{\varepsilon,2}^h)]^{\frac{1}{2}}|\nabla w_{\varepsilon,2}^h|)^2\Big]dt \le C. \tag{73}$$

We can express (73) for $i=1,2$ in the following manner:

$$\frac{\gamma}{2}|\phi_{\varepsilon,i}^h|_1^2+\int_T\Big([M(\phi_{\varepsilon,i}^h)]^{\frac{1}{2}}|\nabla w_{\varepsilon,i}^h|\Big)^2dt \le C, \tag{74}$$

where C is not dependent of T and k. Furthermore, by choosing $\chi^h=1$ in (52) and integrating both sides over the interval $(0,t)$, we obtain that

$$\int_0^t(\partial_s\phi_{\varepsilon,i}^h,1)^h ds = -\int_0^t(M(\phi_{\varepsilon,i}^h)\nabla w_{\varepsilon,i}^h,\nabla 1)=0,\ \ then\int_0^t(\partial_s\phi_{\varepsilon,i}^h,1)^h ds=0.$$

This results in the following outcome:

$$(\phi_{\varepsilon,i}^h(t),1)^h=(\phi_{\varepsilon,i}^h(0),1)^h. \tag{75}$$

Upon observing (75) and (51), it becomes evident that

$$|(\phi_{\varepsilon,i}^h(t),1)^h| = |(\phi_{\varepsilon,i}^h(0),1)^h| = |(P^h\phi_{\varepsilon,i}^0,1)^h| = |(\phi_{\varepsilon,i}^0,1)| \leq C. \tag{76}$$

By applying the discrete Poincare inequality (24), together with (76), (74), and (23), it can be concluded that

$$\|\phi_{\varepsilon,i}^h(t)\|_0 \leq |\phi_{\varepsilon,i}^h(t)|_h \leq C. \tag{77}$$

From (77) and (74), $\forall i = 1,2$, it can be observed that

$$\|\phi_{\varepsilon,i}^h(t)\|_1 = \|\phi_{\varepsilon,i}^h(t)\|_0 + |\phi_{\varepsilon,i}^h(t)|_1 \leq 0, \qquad \forall t, \tag{78}$$

then, the outcomes obtained are as follows:

$$\phi_{\varepsilon,i}^h \in L^\infty(0,T;H^1(\mathfrak{R})). \tag{79}$$

By selecting $\chi^h = \pi^h z$, for all $z \in L^2(0,T;H^1(\mathfrak{R}))$, in equation (52), integrating over the interval $(0,t)$, and employing Hölder's inequality along with (74), we can derive the following:

$$\left|\int_{\mathfrak{R}_T} \partial_t \phi_{\varepsilon,i}^h z d\mathbf{x}dt\right| = -\left|\int_{\mathfrak{R}_T} M(\phi_{\varepsilon,i}^h)\nabla w_{\varepsilon,i}^h, \nabla\pi^h z d\mathbf{x}dt\right| \leq C\|\nabla z\|_{L^2(\mathfrak{R}_T)}. \tag{80}$$

Therefore, it follows that

$$\|\partial_t\phi_{\varepsilon,i}^h\|^2_{L^2(0,T;(H^1(\mathfrak{R})'))} = \sup_{z\neq 0}\frac{|\int_0^T\int_{\mathfrak{R}}\partial_t\phi_i^h z d\mathbf{x}dt|^2}{\|z\|_{L^2(0,T;H^1(\mathfrak{R}))}} < C, \tag{81}$$

which leads to

$$\partial_t\phi_{\varepsilon,i}^h \in L^2(0,T;(H^1(\mathfrak{R}))'), \qquad \forall i = 1,2. \tag{82}$$

To demonstrate the boundedness of $\phi_{\varepsilon,i}^h(t)$ in $L^2(0,T;(H^1(\mathfrak{R}))')$, it is necessary to establish that $\phi_{\varepsilon,i}^h(t) - ⨍\phi_{\varepsilon,i}^h(t)$ belongs to $L^2(0,T;(H^1(\mathfrak{R}))')$. Taking into account (13) and (76), we deduce that

$$\phi_{\varepsilon,i}^h(t) - ⨍\phi_{\varepsilon,i}^h(t) = \phi_{\varepsilon,i}^h(t) - \frac{1}{|\mathfrak{R}|}(\phi_{\varepsilon,i}^h(t),1) = \int_0^t \frac{\partial}{\partial s}\phi_{\varepsilon,i}^h(s)ds + \phi_{\varepsilon,i}^h(0) - \frac{1}{|\mathfrak{R}|}(\phi_{\varepsilon,i}^h(0),1). \tag{83}$$

Therefore, by employing Young's inequality, setting $t = T$ in the integration on the right-hand side, and considering (82) and (18), we can derive that

$$\|\phi_{\varepsilon,i}^h(t) - ⨍\phi_{\varepsilon,i}^h(t)\|_{-1}^2 \leq C\left(\left\|\int_0^T \frac{\partial\phi_{\varepsilon,i}^h}{\partial t}dt\right\|_{-1}^2 + \|\phi_{\varepsilon,i}^h(0)\|_0^2 + \|(\phi_{\varepsilon,i}^h(0),1)\|_0^2\right) \leq C. \tag{84}$$

Upon integrating over the interval $(0,T)$ and utilizing (19), we derive that

$$\left\|\phi_{\varepsilon,i}^h(t) - ⨍\phi_{\varepsilon,i}^h(t)\right\|^2_{L^2(0,T;(H^1(\mathfrak{R}))')} \leq \int_0^T \left\|\phi_{\varepsilon,i}^h(t) - ⨍\phi_{\varepsilon,i}^h(t)\right\|_{-1}^2 dt \leq C\int_0^T dt \leq C(T). \tag{85}$$

Thus, from (82) and (85), it follows that

$$\|\phi^h_{\varepsilon,i}\|^2_{H^1(0,T;(H^1(\mathfrak{R}))')} \leq C. \tag{86}$$

We must now establish that $|w^k_{\varepsilon,i}|_1$ is bounded. This can be achieved by employing the Poincare inequality (24) and (23), leading to

$$\|w^h_{\varepsilon,i}\|^2_0 \leq C_p(|w^h_{\varepsilon,i}|^2_1 + |(w^h_{\varepsilon,i},1)^h|^2). \tag{87}$$

Subsequently, by choosing $\chi^h = 1$ in (53), we obtain that

$$|(w^h_{\varepsilon,i},1)^h| \leq |(\Psi'_{\varepsilon,i}(\phi^h_{\varepsilon,i}),1)^h| + |(f^{(i)}_D(\phi^h_{\varepsilon,1},\phi^h_{\varepsilon,2}),1)^h|. \tag{88}$$

Analogous to (69), we can establish that

$$|(f^{(i)}_D(\phi^h_{\varepsilon,1},\phi^h_{\varepsilon,2}),1)^h \leq C[\|\phi_{\varepsilon,1}\|^2_1+1][\|\phi_{\varepsilon,2}\|^2_1+1] \leq C. \tag{89}$$

By considering (76), (89), and (79) in (88), it follows that

$$|(w^h_{\varepsilon,i},1)^h| \leq C. \tag{90}$$

Upon integrating (87) over $t \in (0,T)$ and taking into account (74) and (90), we arrive at

$$w^h_{\varepsilon,i} \in L^2(0,T;H^1(\mathfrak{R})). \tag{91}$$

Utilizing (37), (38), and the bound (78), we can deduce, for $i = 1,2$ with $i \neq j$, the following:

$$|f^{(i)}_D(\phi^h_{\varepsilon,1},\phi^h_{\varepsilon,2})|^2_h \leq C\|\phi^h_{\varepsilon,i}+\alpha_i\|^2_1\|\phi^h_{\varepsilon,j}+\alpha_j\|^4_1 \quad \leq C. \tag{92}$$

Now, by employing (92), the fact that $|f^{(i)}_D(\phi^h_{\varepsilon,1},\phi^h_{\varepsilon,2})|^2_h = |\pi^h fD^{(i)}(\phi^h_{\varepsilon,1},\phi^h_{\varepsilon,2})|^2_h$, and the equivalence result (23), we derive that

$$\|\pi^h f^{(i)}_D(\phi^h_{\varepsilon,1},\phi^h_{\varepsilon,2})\|_{L^\infty(0,T,L^2(\mathfrak{R}))} \leq C. \tag{93}$$

By applying (53) with $\chi^h = \pi^h \Xi_\varepsilon(\phi^h_{\varepsilon,i}) \in S^h$ and considering (22) along with Young's inequality, we reach

$$\begin{aligned}(w^h_{\varepsilon,i},\pi^h\Xi_\varepsilon(\phi^h_{\varepsilon,i}))^h =&\gamma(\nabla\phi^h_{\varepsilon,i},\nabla\pi^h\Xi_\varepsilon(\phi^h_{\varepsilon,i})) + (\Xi_\varepsilon(\phi^h_{\varepsilon,i}),\pi^h\Xi_\varepsilon(\phi^h_{\varepsilon,i}))^h \\ &- \theta_i(\phi^h_{\varepsilon,i},\pi^h\Xi_\varepsilon(\phi^h_{\varepsilon,i}))^h + f^{(i)}_D(\phi^h_{\varepsilon,1},\phi^h_{\varepsilon,2}),\pi^h\Xi_\varepsilon(\phi^h_{\varepsilon,i}))^h.\end{aligned} \tag{94}$$

From (94), we can deduce that

$$\begin{aligned}\gamma(\nabla\phi^h_{\varepsilon,i},\nabla\pi^h\Xi_\varepsilon(\phi^h_{\varepsilon,i})) + |\pi^h\Xi_\varepsilon(\phi^h_{\varepsilon,i})|^2_h =&\frac{1}{2}|\pi^h\Xi_\varepsilon(\phi^h_{\varepsilon,i})|^2_h \\ &+ C\Big[|w^h_{\varepsilon,i}|^2_h + |\phi^h_{\varepsilon,i}|^2_h + |\pi^h f^{(i)}_D(\phi^h_{\varepsilon,1},\phi^h_{\varepsilon,2})|^2_h\Big].\end{aligned} \tag{95}$$

By applying Lemma 2, the first term on the left-hand side of (94) is non-negative. Consequently, we deduce the estimate (60) after integrating the expression over $(0,T)$ and considering the bounds (56), (57), and (59). □

Theorem 2. *Under the assumptions of Theorem 1, there exists a solution $\phi_1^h, \phi_2^h, w_1^h, w_2^h$ to (Q^h) such that the following stability estimates hold independently of h:*

$$\phi_i^h \in L^\infty(0,T;(H^1(\mathfrak{R}))\cap H^1(0,T;(H^1(\mathfrak{R}))'), \tag{96}$$
$$w_i^h \in L^2(0,T;H^1(\mathfrak{R})), \tag{97}$$
$$\partial_t\phi_i^h \in L^2(0,T;(H^1(\mathfrak{R}))'), \tag{98}$$
$$\pi^h f_D^{(i)}(\phi_1^h,\phi_2^h) \in L^\infty(0,T,L^2(\mathfrak{R})), \tag{99}$$
$$\pi^h\Xi(\phi_i^h) \in L^2(\mathfrak{R}_T). \tag{100}$$

Proof. The proof of this theorem can be accomplished using the bounds (56)-(58) and (60). □

(A_2) Let $\{\phi_1^0,\phi_2^0\} \in H^2(\mathfrak{R})\times H^2(\mathfrak{R}), |\Delta\phi_1^0|_1 + |\Delta\phi_2^0|_1 \leq C, \frac{\partial\phi_1^0}{\partial\nu} = \frac{\partial\phi_2^0}{\partial\nu} = 0$ on $\partial\mathfrak{R}$, and

$$\max\{|\phi_1^0|_{0,\infty}, |\phi_2^0|_{0,\infty}\} \leq 1-\delta_0,$$

for some given $\delta_0 \in (0,1)$.

Theorem 3. *Assuming that both (A_2) and (A^h) are satisfied, and letting $\phi_i^{h,0} = P_\gamma^h\phi_i^0$ for $i=1,2$, then for all $\varepsilon \leq \min\varepsilon_0, \frac{\delta_0}{2}$ and for all $h \leq h_*$, the solution of $(\mathrm{Q}_\varepsilon^h)$ ensures the following additional stability estimates, which are independent of the parameters ε and h:*

$$\|\partial_t\phi_{\varepsilon,i}^h\|_{L^2(0,T;H^1(\mathfrak{R}))} + \|\partial_t\phi_{\varepsilon,i}^h\|_{L^\infty(0,T;(H^1(\mathfrak{R}))')} \leq C, \tag{101}$$
$$\|w_{\varepsilon,i}^h\|_{L^\infty(0,T;H^1(\mathfrak{R}))} + \|\pi^h\Xi_\varepsilon(\phi_{\varepsilon,i}^h)\|_{L^\infty(0,T;L^2(\mathfrak{R}))} \leq C. \tag{102}$$

Proof. This theorem can be proven by following the standard steps used to prove the error of the semi-discrete approximation of the finite element method. □

6 A fully -discrete approximation

We define the time increment as $\Delta t = \frac{T}{N}$, where N is a positive integer. In our fully linear finite element approximation, we discretize the nonlinearities Ψ_i and $f_D^{(i)}$, where $i=1,2$, at discrete time levels $t = t_n = n\Delta t$ for $n = 1,\ldots,N$. These functions are expressed in terms of Φ_i^n and Φ_i^{n-1}, where Φ_i^n is an approximation of the continuous solution ϕ_i at the time $t=t_n$. The discretization for the nonlinearities is as follows: For $i=1,2$, we approximate the logarithmic term in (Q), $\Psi_i'(\Phi_i) = \Xi(\Phi_i) - \theta_i\Phi_i$, as

$$\Xi(\Phi_i^n) - \mu\theta_i\Phi_i^n - (1-\mu)\theta_i\Phi_i^{n-1}, \quad \mu \in [0,\frac{1}{2}], \tag{103}$$

and we approximate the D-coupling term, $f_D^{(i)}(\Phi_1,\Phi_2) = 2D(\phi_i+\alpha_i)(\phi_j+\alpha_j)$ as

$$D(\Phi_i^n+\alpha_i)[(\Phi_j^n+\alpha_j)^2 + (\Phi_j^{n-1}+\alpha_j)^2], \quad i,j=1,2 \text{ with } i\neq j. \tag{104}$$

For the sake of convenient notation, we introduce $\bar{f}^{(i)}_{n,n-1}$, defined as follows:

$$\bar{f}^{(i)}_{n,n-1} = 2D(\Phi^n_i + \alpha_i)(\Phi^{n-1}_j + \alpha_j)^2, \quad i,j = 1,2 \text{ with } i \neq j, \tag{105}$$

$$i.e.\ \ \bar{f}^{(1)}_{n,n-1} = f^{(1)}_D(\Phi^n_1, \Phi^{n-1}_2),\ \ \bar{f}^{(2)}_{n,n-1} = f^{(2)}_D(\Phi^{n-1}_1, \Phi^n_2). \tag{106}$$

Based on equations (104) and (105), the D-coupling term can be expressed as follows:

$$\frac{1}{2}[f^{(i)}_D(\Phi^n_1, \Phi^n_2) + \bar{f}^{(i)}_{n,n-1}], \quad i = 1,2. \tag{107}$$

Hence, given $\mu \in [0, \frac{1}{2}]$ and $\phi^{h,0}_i \in S^h_{m_i}$, we contemplate the subsequent coupled fully-discrete linear finite element approximation of equation (Q):

$(\mathrm{Q}^{h,\Delta t}_{\mu})$ For $n = 1, \ldots, N$ find $\{\Phi^n_1, \Phi^n_2, W^n_1, W^n_2\} \in S^h_{m_1} \times S^h_{m_2} \times S^h \times S^h$ such that $\Phi^0_i = \phi^{h,0}_i, i = 1,2$, and for all $\chi \in S^h$,

$$\Big(\frac{\Phi^n_i - \Phi^{n-1}_i}{\Delta t}, \chi\Big)^h = -(M(\Phi^{n-1}_i)\nabla W^n_i, \nabla\chi), \tag{108}$$

$$\begin{aligned}(W^n_i, \chi)^h = {} & \gamma(\nabla\Phi^n_i, \nabla\chi) + (\Xi(\Phi^n_i) - \mu\theta_i\Phi^n_i - (1-\mu)\theta_i\Phi^{n-1}_i, \chi)^h \\ & + \frac{1}{2}(f^{(i)}_D(\Phi^n_1, \Phi^n_2) + \bar{f}^{(i)}_{n,n-1}, \chi)^h.\end{aligned} \tag{109}$$

The corresponding regularized version of $(\mathrm{Q}^{h,\Delta t}_{\mu})$, for given $\mu \in [0, \frac{1}{2}]$ and $\phi^{h,0}_i \in S^h_{m_i}$ is

$(\mathrm{Q}^{h,\Delta t}_{\mu,\varepsilon})$ For $n = 1, \ldots, N$ find $\{\Phi^n_{\varepsilon,1}, \Phi^n_{\varepsilon,2}, W^n_{\varepsilon,1}, W^n_{\varepsilon,2}\} \in S^h_{m_1} \times S^h_{m_2} \times S^h \times S^h$ such that $\Phi^0_{\varepsilon,i} = \phi^{h,0}_i$, $i = 1,2$, and for all $\chi \in S^h$

$$\Big(\frac{\Phi^n_{\varepsilon,i} - \Phi^{n-1}_{\varepsilon,i}}{\Delta t}, \chi\Big)^h = -(M(\Phi^{n-1}_{\varepsilon,i})\nabla W^n_{\varepsilon,i}, \nabla\chi), \tag{110}$$

$$\begin{aligned}(W^n_{\varepsilon,i}, \chi)^h = {} & \gamma(\nabla\Phi^n_{\varepsilon,i}, \nabla\chi) + (\Xi_\varepsilon(\Phi^n_{\varepsilon,i}) - \mu\theta_i\Phi^n_{\varepsilon,i} - (1-\mu)\theta_i\Phi^{n-1}_{\varepsilon,i}, \chi)^h \\ & + \frac{1}{2}(f^{(i)}_D(\Phi^n_{\varepsilon,1}, \Phi^n_{\varepsilon,2}) + \bar{f}^{(i)}_{\varepsilon,n,n-1}, \chi)^h,\end{aligned} \tag{111}$$

where $\bar{f}^{(1)}_{\varepsilon,n,n-1} = f^{(1)}_D(\Phi^n_{\varepsilon,1}, \Phi^{n-1}_{\varepsilon,2})$, $\ \bar{f}^{(2)}_{\varepsilon,n,n-1} = f^{(2)}_D(\Phi^{n-1}_{\varepsilon,1}, \Phi^n_{\varepsilon,2})$.

6.1 Existence of a fully-discrete approximation

In this segment, we demonstrate the existence of a solution for the problem $(\mathrm{Q}^{h,\Delta t}_{\mu,\varepsilon})$ by employing a method akin to the one utilized in [1, 12, 13] to establish the existence of a linear finite element approximation for a cross-diffusion equation. This method hinges on creating a contradiction to the Schauder fixed point theorem.

Theorem 4. *Let the assumptions of Theorem 1 hold with $\phi^{h,0}_i = P^h\phi^0_i$ or $\phi^{h,0}_i = P^h_\gamma\phi^0_i, i = 1,2$. Then for all $\mu \in [0, \frac{1}{2}]$, for all $\varepsilon \leq \varepsilon_0$, for all $h > 0$ and for all $\Delta t > 0$ there exists a solution $\{\Phi^n_{\varepsilon,1}, \Phi^n_{\varepsilon,2}, W^n_{\varepsilon,1}, W^n_{\varepsilon,2}\} \in S^h_{m_1} \times S^h_{m_2} \times S^h \times S^h$ to $(\mathrm{Q}^{h,\Delta t}_{\mu,\varepsilon})$, for $n = 1, \ldots, N$.*

Theorem 5. *Let the assumptions of Theorem 4 hold with $\phi_i^{h,0} = P^h \phi_i^0$. Then for all $\mu \in [0,1]$, for all $\varepsilon \le \varepsilon_0$, for all $h > 0$ and for all $\Delta t > 0$ and $M_{\varepsilon,i\max} \ge \max_{n=1\to N} M_{\varepsilon,i\max}^{n-1}$ and $M_{\varepsilon,i\max}^{n-1} = \|M(\Phi_{\varepsilon,i}^{n-1})\|_{0,\infty}$ a solution $\{\Phi_{\varepsilon,1}^n, \Phi_{\varepsilon,2}^n, W_{\varepsilon,1}^n, W_{\varepsilon,2}^n\}$ to the n-th step of $(\mathrm{Q}_{\mu,\varepsilon}^{h,\Delta t})$ is such that*

$$\max_{n=1\to N}\left[\|\Phi_{\varepsilon,1}^n\|_1^2 + \|\Phi_{\varepsilon,2}^n\|_1^2\right] + \sum_{n=1}^{N}[\|\Phi_{\varepsilon,1}^n - \Phi_{\varepsilon,1}^{n-1}\|_1^2 + \|\Phi_{\varepsilon,2}^n - \Phi_{\varepsilon,2}^{n-1}\|_1^2] \le C, \tag{112}$$

$$\Delta t \sum_{n=1}^{N}\left[\|[M(\Phi_{\varepsilon,1}^{n-1})]^{\frac{1}{2}}\nabla W_{\varepsilon,1}^n\|_0^2 + \|[M(\Phi_{\varepsilon,2}^{n-1})]^{\frac{1}{2}}\nabla W_{\varepsilon,2}^n\|_0^2\right] \le C, \tag{113}$$

$$\Delta t \sum_{n=1}^{N}\left([M_{\varepsilon,1}{}_{max}^{n-1}]^{-1}|\hat{\mathscr{G}}^h(\frac{\Phi_{\varepsilon,1}^n - \Phi_{\varepsilon,1}^{n-1}}{\Delta t})|_1^2 + [M_{\varepsilon,2}{}_{max}^{n-1}]^{-1}|\hat{\mathscr{G}}^h(\frac{\Phi_{\varepsilon,2}^n - \Phi_{\varepsilon,2}^{n-1}}{\Delta t})|_1^2\right) \le C. \tag{114}$$

The above theorems can be proven by following a technique similar to what was adopted in [1,12,13].

7 Numerical results

To validate the theoretical findings and demonstrate the effectiveness of the linear finite element approximation, numerical simulations were conducted in this section. Programs written in the Matlab programming language were employed for all simulations. Subsequently, numerical simulations are carried out in both one and two space dimensions. The results of the fully-discrete system in one and two space dimensions are then provided and analyzed.

7.1 Error computations

To assess the error, we modify problem (Q) by incorporating source terms $f_i(\mathbf{x},t), h_i(\mathbf{x},t), i = 1,2$. This results in the reformulation of system (11)-(12) into the following form:

$$\partial_t \phi_i = \nabla(M(\phi_i)\nabla w_i) + f_i(\mathbf{x},t), \tag{115}$$

$$w_i = -\gamma\Delta\phi_i + \Psi_i'(\phi_i) + f_D^{(i)}(\phi_1,\phi_2) + h_i(\mathbf{x},t). \tag{116}$$

7.1.1 One-dimensional error

Here, we present a representative simulation of solution for the system (115)-(116) by using linear finite element approximation. This example adhere to Dirichlet boundary conditions. Specifically, we chose parameters such as $\theta = \theta_1 = \theta_2 = \sigma_1 = \sigma_1 = D = 1, \gamma = 0.0025, T = 1$, and $\Omega = [0,1]$ for simplicity. The initial and boundary conditions, along with the source terms $f_1(x,t), f_2(x,t), h_1(x,t)$, and $h_2(x,t)$, are derived from the relevant analytical solution for each case.

To initiate the simulations, we partition the domain $\Omega = [0,1]$ into J uniform intervals, with a mesh size set to $h = 1/J$. The analytical solution considered in this simulations are as follows: $\phi_1 = 0.5\exp(-t)\cos(\pi x)$, $w_1 = 0.25\exp(-t)\cos(2\pi x)$, $\phi_2 = 0.5\exp(-t)\cos(3\pi x)$, $w_2 = 0.25\exp(-t)\cos(4\pi x)$.

Tables 1 and 2 present theL^1, L^2, and L^∞ norm errors for the two test cases. The error values are computed with $M(\phi_i) = 1$ and $1-\phi_i^2$ for $i = 1,2$, respectively. The results show that as J increases, corresponding to a decrease in the mesh size h, the errors consistently decrease. This trend demonstrates the convergence of the numerical method with finer mesh resolution.

Table 1: The errors of linear finite element approximation in the L^1, L^2, and L^∞ norms for the one-dimensional problem with homogeneous Dirichlet boundary conditions which are calculated for $M(\phi_i) = 1, i = 1,2$ with $\theta = \theta_1 = \theta_2 = \sigma_1 = \sigma_1 = D = 1, \gamma = 0.0025, T = 1$, and $\Omega = [0,1]$.

J	$\lVert e - E_\varepsilon \rVert$			$\lVert s - S_\varepsilon \rVert$		
	L^1	L^2	L^∞	L^1	L^2	L^∞
10	3.20E-02	1.25E-02	5.76E-02	8.32E-02	2.95E-02	1.19E-01
20	8.68E-03	2.24E-03	1.49E-02	2.09E-02	5.31E-03	4.14E-02
25	5.63E-03	1.29E-03	1.04E-02	1.34E-02	3.08E-03	2.92E-02
40	2.24E-03	4.06E-04	4.57E-03	5.32E-03	9.70E-04	1.30E-02
50	1.44E-03	2.34E-04	3.03E-03	3.42E-03	5.59E-04	8.64E-03

Table 2: The errors of linear finite element approximation in the L^1, L^2, and L^∞ norms for the one-dimensional problem with homogeneous Dirichlet boundary conditions which are calculated for $M(\phi_i) = 1 - \phi_i^2, i = 1,2$ with $\theta = \theta_1 = \theta_2 = \sigma_1 = \sigma_1 = D = 1, \gamma = 0.0025, T = 1$, and $\Omega = [0,1]$.

J	$\lVert e - E_\varepsilon \rVert$			$\lVert s - S_\varepsilon \rVert$		
	L^1	L^2	L^∞	L^1	L^2	L^∞
10	4.58E-02	1.74E-02	8.03E-02	8.02E-02	3.14E-02	1.53E-01
20	1.84E-02	5.03E-03	5.18E-02	2.12E-02	5.62E-03	4.79E-02
25	1.43E-02	3.48E-03	4.22E-02	1.39E-02	3.26E-03	3.08E-02
40	8.58E-03	1.64E-03	2.64E-02	5.62E-03	1.04E-03	1.34E-02
50	6.78E-03	1.15E-03	2.10E-02	3.64E-03	6.08E-04	9.84E-03

7.2 One-dimensional simulations

In the context of one-dimensional spatial simulations within the domain $\Omega = [0,1]$, computations were conducted over the time interval $0 \leq t \leq T$, utilizing mesh points $x_j = jh$ for $j = 0,\ldots,J$, where $h = L/J$. The simulations were performed with Neumann boundary conditions, and the initial conditions were specified as $\phi^0 i = \hat{\zeta}(\cos(\pi x) - \cos(3\pi x))$ for $i = 1,2$, where $\hat{\zeta}_1$ and $\hat{\zeta}_2$ are small. Four simulations were executed for the purpose of comparing numerical approximations, with default parameters set as follows unless explicitly stated otherwise: $\theta_1 = \theta_2 = \sigma_1 = \sigma_1 = 1$, $\mu = D = 0.5$, $\gamma = 0.005$, $J = 50$, $\hat{\zeta}_1 = 0.0001$, $\hat{\zeta}_2 = 0.0002$, and $\Omega = [0,1]$. The numerical results were obtained for two cases: $M(\phi_i) = 1$ and $M(\phi_i) = 1 - \phi_i^2$.

In the initial experiment, parameters were set to $\hat{\zeta}_1 = 0.0001$, $\hat{\zeta}_2 = 0.0002$, and $\theta = 0.8$. Notably, the numerical solutions exhibited growth with the passage of time. A parallel trend was observed in the second experiment, where the same data was employed, except for setting $\theta = 0.5$. The early-stage results of these two experiments are visually presented in Figure 1.

In the third experimental iteration, parameters were set to $\hat{\zeta}_1 = 0.0001$, $\hat{\zeta}_2 = 0.0002$, and $\theta = 0.8$. Interestingly, in this experiment, it was observed that the numerical solutions did not exhibit an increase over time, as depicted in Figure 2 (a) and (b). Subsequently, the third experiment was repeated with

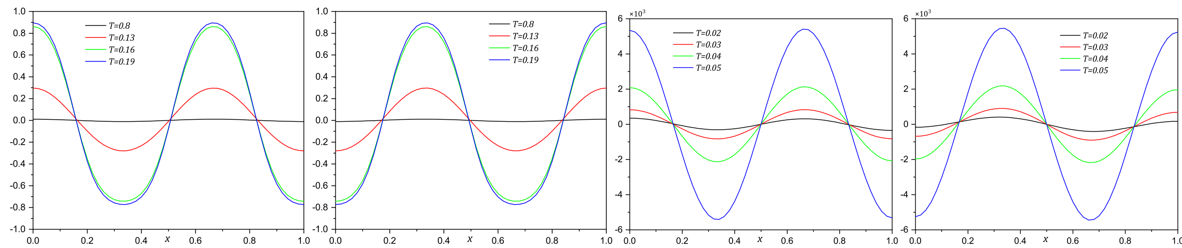

(a) $\Phi_{\varepsilon,1}$, $\theta = 0.8$ **(b)** $\Phi_{\varepsilon,2}$, $\theta = 0.8$ **(c)** $\Phi_{\varepsilon,1}$, $\theta = 0.5$ **(d)** $\Phi_{\varepsilon,2}$, $\theta = 0.5$

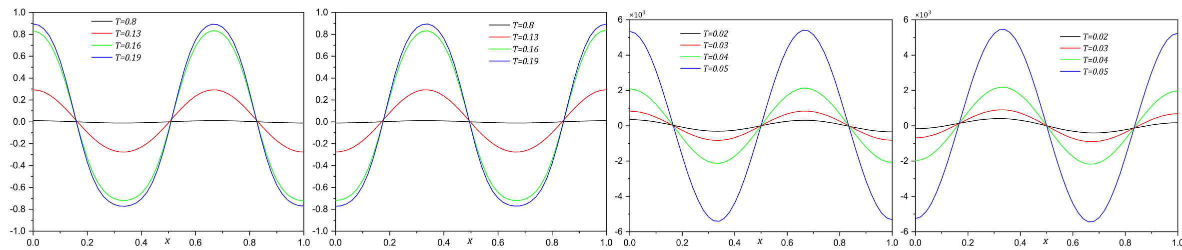

(e) $\Phi_{\varepsilon,1}$, $\theta = 0.8$ **(f)** $\Phi_{\varepsilon,2}$, $\theta = 0.8$ **(g)** $\Phi_{\varepsilon,1}$, $\theta = 0.5$ **(h)** $\Phi_{\varepsilon,2}$, $\theta = 0.5$

Figure 1: Numerical solutions by using linear finite element approximation at different time levels. $\theta_1 = \theta_2 = \sigma_1 = \sigma_1 = 1, \mu = D = 0.5, \gamma = 0.005, J = 50, \phi_i^0 = \hat{\zeta}(\cos(\pi x) - \cos(3\pi x)), i = 1, 2,$ $\hat{\zeta}_1 = 0.0001, \hat{\zeta}_2 = 0.0002$, and $\Omega = [0, 1]$. In (a), (b), (c), and (d), we choose $M(\phi_i) = 1$, whereas in (e), (f), (g), and (h), we opt for $M(\phi_i) = 1 - \phi_i^2$.

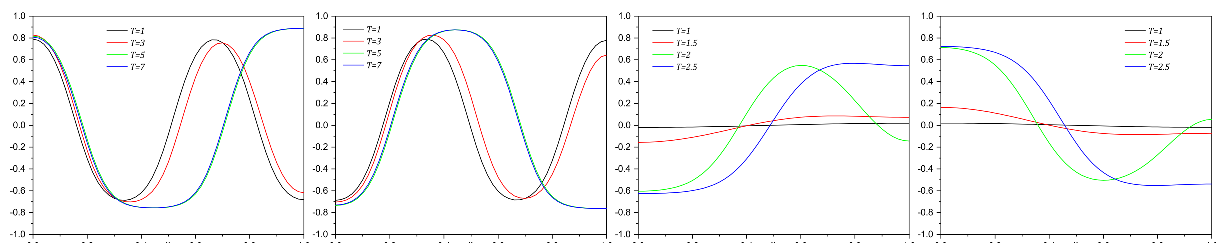

(a) $\Phi_{\varepsilon,1}$, $D = 0.5$ **(b)** $\Phi_{\varepsilon,2}$, $D = 0.5$ **(c)** $\Phi_{\varepsilon,1}$, $D = 0.2$ **(d)** $\Phi_{\varepsilon,2}$, $D = 0.2$

Figure 2: Numerical solutions by using linear finite element approximation at different time levels. $\theta = 0.98, \theta_1 = \theta_2 = \sigma_1 = \sigma_1 = 1, \mu = 0.5, \gamma = 0.005, J = 50, \phi_i^0 = \hat{\zeta}_i(\cos(\pi x) - \cos(3\pi x)), i = 1, 2,$ $\hat{\zeta}_1 = 0.001, \hat{\zeta}_2 = 0.002,$ $M(\phi_i) = 1 - \phi_i^2$ and $\Omega = [0, 1]$.

identical parameters, except for $D = 0.2$. In contrast, this time the numerical solutions displayed a reduction to zero as time progressed, as illustrated in Figure 2 (c) and (d). Furthermore, it was noted that solutions underwent a significantly faster evolution when θ deviated substantially from both θ_1 and θ_2.

7.3 Two-dimensional simulations

In this section, we employed the domain $\Omega = [0, L]^2$ and implemented a square uniform mesh with vertices $(x_i, y_j) = (ih, jh)$, where $i, j = 0, \ldots, J$. Here, $h = L/J$ denotes the uniform spacing in both the x and y directions. The mesh was generated using a 'right-angled' triangulation, dividing each square

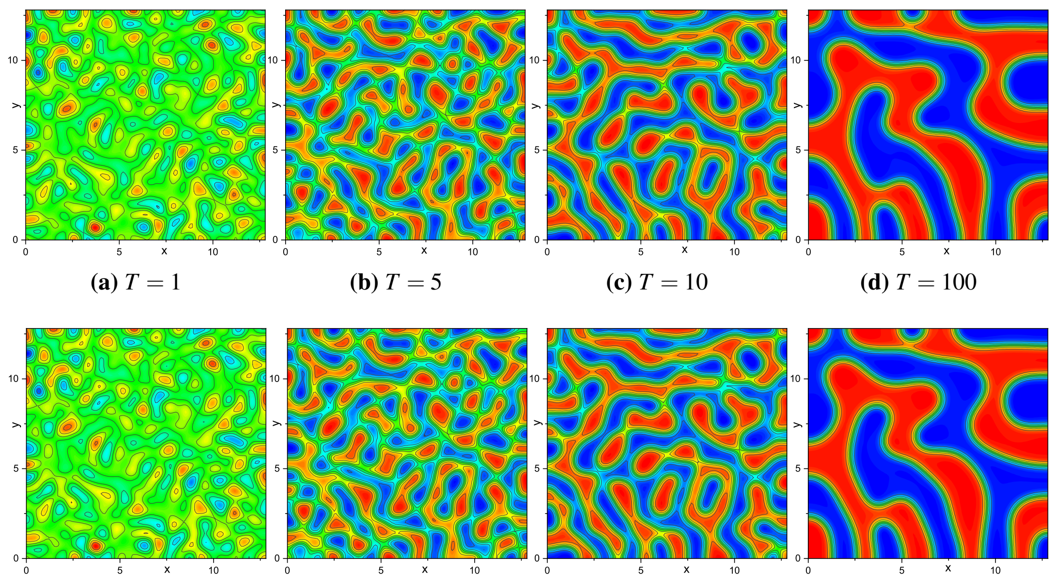

(a) $T = 1$ **(b)** $T = 5$ **(c)** $T = 10$ **(d)** $T = 100$

(e) $T = 1$ **(f)** $T = 5$ **(g)** $T = 10$ **(h)** $T = 100$

Figure 3: Evolution of the concentration $\phi_1(x,y,t)$ with $\theta = 1, \theta_1 = \theta_2 = \sigma_1 = \sigma_1 = 0.1, D = 0, \gamma = 0.0025, \phi_i^0 = 0.1(2\text{rand}() - 1), i = 1,2$, and $\Omega = [0,12.8] \times [0,12.8]$. In (a), (b), (c), and (d), we choose $M(\phi_i) = 1$, whereas in (e), (f), (g), and (h), we opt for $M(\phi_i) = 0.5 * (1 - \phi_i^2)$.

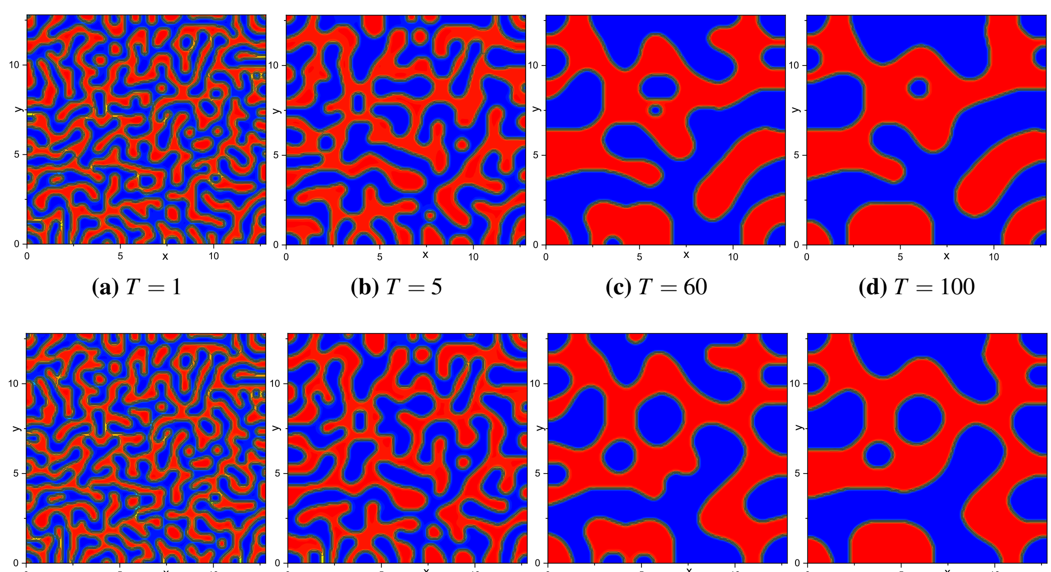

(a) $T = 1$ **(b)** $T = 5$ **(c)** $T = 60$ **(d)** $T = 100$

(e) $T = 1$ **(f)** $T = 5$ **(g)** $T = 60$ **(h)** $T = 100$

Figure 4: Evolution of the concentration $\phi_1(x,y,t)$ with a constant mobility $\theta = 1, \theta_1 = \theta_2 = \sigma_1 = \sigma_1 = 0.1, D = 0.5, \gamma = 0.0025, \phi_i^0 = 0.1(2\text{rand}() - 1), i = 1,2$, and $\Omega = [0,12.8] \times [0,12.8]$. In (a), (b), (c), and (d), we choose $M(\phi_i) = 1$, whereas in (e), (f), (g), and (h), we opt for $M(\phi_i) = 0.5 * (1 - \phi_i^2)$.

with a diagonal running from the top-right corner to the bottom-left corner. Nodes were ordered in the 'natural way,' with sequential numbering from left to right, starting from the bottom row.

For our simulations, we conducted two experiments, solving the problem across the domain $\Omega = [0,12.8]\times[0,12.8]$ with a mesh spacing of $h = 0.1$, a time step of $\Delta t = 0.0001$, and a total of $J = 1280$ nodes. The considered initial conditions are $\phi_i^0 = 0.1(2\text{rand}()-1), \quad i = 1,2$. The constants for the problem were chosen as follows: $\theta = 1, \theta_1 = \theta_2 = \sigma_1 = \sigma_1 = 0.1, D = 0, \gamma = 0.0025, \phi_i^0 = 0.1(2\text{rand}()-1)$ for $i = 1,2$, and $\Omega = [0,12.8]\times[0,12.8]$. In all figures, the nondegenerate mobility function $M(\phi_i) = 1$ for $i = 1,2$ was selected in (a), (b), (c), and (d), while in (e), (f), (g), and (h), we chose $M(\phi_i) = 0.5*(1-\phi_i^2)$. The concentration evolution $\phi_1(x,y,t)$ is depicted at various time levels in Figures 3-4.

Acknowledgments

We would like to express our gratitude to an anonymous referee for his valuable feedback and insightful comments, which have greatly contributed to the enhancement of this manuscript.

References

[1] G.A. Al-Juaifri, A.J. Harfash, *Finite element analysis of nonlinear reaction–diffusion system of fitzhugh–nagumo type with robin boundary conditions*, Math. Comput. Simul. **203** (2023) 486–517.

[2] J.W. Barrett, J.F. Blowey, *An optimal error bound for a finite element approximation of a model for phase separation of a multi-component alloy with non-smooth free energy*, ESAIM: Math. Model. Numer. Anal. **33** (1999) 971–987.

[3] J.W. Barrett, J.F. Blowey, *Finite element approximation of an Allen–Cahn/Cahn–Hilliard system*, IMA J. Numer. Anal. **22** (2002) 11–71.

[4] J.W. Cahn, J.E. Hilliard, *Free energy of a nonuniform system. I. interfacial free energy*, J. Chem. Phys. **28** (1958) 258–267.

[5] T. Cazenave, *Semilinear Schrodinger Equations*, American Mathematical Society, 2003.

[6] J. Ciavaldini, *Analyse numerique dun probleme de stefan adeux phases par une methode delements finis*, SIAM J. Numer. Anal. **12** (1975) 464–487.

[7] C.M. Elliott, H. Garcke, *On the Cahn–Hilliard equation with degenerate mobility*, SIAM J. Math. Anal. **27** (1996) 404–423.

[8] C.M. Elliott, S. Luckhaus, *A generalised diffusion equation for phase separation of a multi-component mixture with interfacial free energy*, MA, Uniersity of Minnesota, preprint 887, 1991.

[9] H. Gomez, V. M. Calo, Y. Bazilevs, T.J. Hughes, *Isogeometric analysis of the Cahn–Hilliard phase-field model*, Comput. Methods Appl. Mech. Eng. **197** (2008) 4333–4352.

[10] J.D. Gunton, R. Toral, A. Chakrabarti, *Numerical studies of phase separation in models of binary alloys and polymer blends*, Phys. Scripta **33** (1990) 12–19.

[11] N. Habibi and A. Mesforush, *Semi-algebraic mode analysis for multigrid method on regular rectangular and triangular grids*, J. Math. Model. **11** (2023) 547–572.

[12] S.M. Hassan, A.J. Harfash, *Finite element analysis of a two-species chemotaxis system with two chemicals*, Appl. Numer. Math. **182** (2022) 148–175.

[13] S.M. Hassan, A.J. Harfash, *Finite element approximation of a keller–segel model with additional self-and cross-diffusion terms and a logistic source*, Commun. Nonlinear Sci. Numer. Simul. **104** (2022) 106063.

[14] Y. He, Y. Liu, T. Tang, *On large time-stepping methods for the Cahn–Hilliard equation*, Appl. Numer. Math. **57** (2007) 616–628.

[15] M. Izadi, M. Afshar, *Solving the basset equation via chebyshev collocation and ldg methods*, J. Math. Model. **9** (2021) 61–79.

[16] M. Jalili, R. Salehi, *The approximate solution of one dimensional stochastic evolution equations by meshless methods*, J. Math. Model. **9** (2021) 599–609.

[17] J. Kim, K. Kang, *A numerical method for the ternary Cahn–Hilliard system with a degenerate mobility*, Appl. Numer. Math. **59** (2009) 1029–1042.

[18] J. Langer, M. Bar-On, H.D. Miller, *New computational method in the theory of spinodal decomposition*, Phys. Rev. A **11** (1975) 1417.

[19] A. Mesforush, S. Larsson, *A posteriori error analysis for the Cahn-Hilliard equation*, J. Math. Model. **10** (2022) 437–452.

[20] L. Modica, *The gradient theory of phase transitions and the minimal interface criterion*, Arch. Rational Mech. Anal. **98** (1987) 123–142.

[21] M. Mohammed, T. Mouhcine, *A finite element approximation of a current-induced magnetization dynamics model*, J. Math. Model. **10** (2022) 53–69.

[22] D.M. Saylor, C.-S. Kim, D.V. Patwardhan, J.A. Warren, *Diffuse-interface theory for structure formation and release behavior in controlled drug release systems*, Acta Biomater. **3** (2007) 851–864.

[23] S. Tremaine, *On the origin of irregular structure in saturn's rings*, Astrophys. J. **125** (2003) 894.